

Author's Accepted Manuscript

Fast and efficient VUV/UV emissions from
(Ba,La)F₂: Er crystals

Andrzej J. Wojtowicz, Sebastian Janus, Dawid Piatkowski

PII: S0022-2313(09)00102-1
DOI: doi:10.1016/j.jlumin.2009.01.020
Reference: LUMIN 9613

To appear in: *Journal of Luminescence*

Received date: 4 July 2008
Revised date: 8 December 2008
Accepted date: 6 January 2009

Cite this article as: Andrzej J. Wojtowicz, Sebastian Janus and Dawid Piatkowski, Fast and efficient VUV/UV emissions from (Ba,La)F₂: Er crystals, *Journal of Luminescence* (2009), doi:10.1016/j.jlumin.2009.01.020

This is a PDF file of an unedited manuscript that has been accepted for publication. As a service to our customers we are providing this early version of the manuscript. The manuscript will undergo copyediting, typesetting, and review of the resulting galley proof before it is published in its final citable form. Please note that during the production process errors may be discovered which could affect the content, and all legal disclaimers that apply to the journal pertain.



www.elsevier.com/locate/jlumin

Fast and efficient VUV/UV emissions from (Ba,La)F₂:Er crystals

Andrzej J. Wojtowicz^{1,*}, Sebastian Janus¹ and Dawid Piatkowski¹

¹ Instytut Fizyki, Uniwersytet M. Kopernika, ul. Grudziadzka 5, 87-100 Torun, Poland

* Corresponding author: andywojt@fizyka.umk.pl

Abstract.

We report observation of fast and efficient VUV/UV luminescence from the mixed (Ba,La)F₂:Er crystals. The broad bands, peaking at 162.5, 181.9, 194.2, 202.8, 216.1, 233.5 and 281.5 nm and decaying, at 10 K and 293 K, with time constants of 46 ns and 35 ns respectively, are due to spin-allowed transitions from the low-spin (LS) state of the 4f¹⁰5d configuration.

We also observed a weak and slow broad band emission peaking at 170 nm due to the spin-forbidden transition from the high spin (HS) state of the 4f¹⁰5d configuration.

While at room temperature the excitation into any of the three identified LS bands (J = 8, 7 and 6) dominating the excitation spectrum yields fast VUV and UV emissions, at 10 K the excitation into higher lying J = 7 and 6 bands generates slow and sharp line emissions. The positions of these lines fit energies of transitions originating from the ²G_{7/2} multiplet at 66140 cm⁻¹. The emission from the ²G_{7/2} multiplet has been never, to the best of our knowledge, observed before.

The efficient and fast VUV and UV emissions from the higher (LS, J = 8) with almost no contribution from the lower (HS, J = 8) level of the 4f¹⁰5d configuration are possible because the modified crystal field in (Ba,La)F₂ shifts the level of the (LS, J = 8) state below the ²F_{5/2} multiplet which, therefore, does not contribute to nonradiative relaxation between the LS and HS levels.

We conclude that the ²G_{7/2} and ²F_{5/2} levels have major impact on VUV and UV emissions from the Er³⁺ ion in (Ba,La)F₂ contributing to complex emission pattern described in this report. Their key role, elucidated by the VUV and UV luminescence spectroscopy, is consistent with predictions from a simple configuration coordinate model based on experimental results and calculations of the 4f¹¹ energy levels.

PACS codes: 29.40.Mc; 71.20.Ps; 71.35.-y; 78.55.Hx; 78.60.-b

Key words: (Ba,La)F₂:Er; VUV emission; VUV spectroscopy; Er³⁺ ion

1. Introduction

Although there is a number of applications that could employ efficient and fast VUV and UV emissions from solid state materials (scintillators, tunable VUV/UV solid state lasers, VUV/UV phosphors) there still is a gap between well established and reliable theoretical calculations and scarce experimental results, especially in the VUV spectral range.

In this paper we report experimental studies of VUV and UV luminescence from Er activated mixed crystals of (Ba,Lu)F₂ using wavelength selective synchrotron excitation. The results that we have obtained confirm and extend earlier studies of other fluorides [1].

2. Crystals and experimental set-ups

The mixed crystals of (Ba,Lu)F₂ (30% Lu), have been grown by Optovac Inc (North Brookfield, MA, USA) using the Bridgman method. All of the experiments were performed on the crystals cut from the boule for which the concentration of Er-dopant in the melt was 0.2 mole %. The samples were not subjected to any chemical reducing procedure. They were of high optical quality, clear, displayed no color, no inclusions and no indication of oxygen contamination.

The VUV/UV experiments (luminescence and excitation spectra) were conducted at the SUPERLUMI station of HASYLAB, located at the Doris III storage ring in DESY, Hamburg, Germany. A detailed description of SUPERLUMI's experimental facilities was given by Zimmerer [2] and is also available on-line [3].

For excitation we have used a primary 2 m normal incidence monochromator in 15° McPherson mounting, equipped with the holographic concave grating (1200 grooves/mm), coated by Al+MgF₂ (50-330 nm). The resolution was 0.28 nm.

For emission we have used two monochromators: the home-made 0.5 meter Pouey VUV monochromator (f/2.8, resolution 1.1 nm), equipped with the solar blind Hamamatsu R6836 photomultiplier (115-300 nm) for VUV, and the Acton Research 0.3 m Czerny-

Turner monochromator “Spectra Pro 300i” (f/4, resolution dependent on adjustable slit and a grating), equipped with the Hamamatsu R6358P photomultiplier (200-800 nm) for longer wavelengths spectra.

3. Experimental results and discussion

In Fig. 1 we present the excitation spectrum of the well known green Er^{3+} emission ($^4\text{S}_{3/2} \rightarrow ^4\text{I}_{15/2}$) peaking at 550 nm, measured at 10 K. The three dominant broad bands peaking at 157, 148 and 138 nm correspond, most likely, to spin allowed interconfigurational transitions between the ground state of the $4f^{11}$ configuration ($^4\text{I}_{15/2}$) and three excited states of the $4f^{10}5d$ configuration [4]. These $4f^{10}5d$ states involve the lowest energy crystal field split 5d state and the three lowest $4f^{10}$ states, $^5\text{I}_8$, $^5\text{I}_7$ and $^5\text{I}_6$, respectively. In the case of the spin-forbidden transition ($\Delta S = 1$) the final state must have either $S = 1/2$ (higher energy doublets) or $S = 5/2$ (lower energy sextets). The most likely candidate for such a spin-forbidden transition is a weak broad band at 165 nm shown in Fig. 1, labeled (HS, $J = 8$) and identified as the lowest high spin (HS) state (sextet) $4f^{10}(^5\text{I}_8)5d$.

The arrows indicate the positions of levels due to the states of $4f^{11}$ configuration. The energies of these levels have been calculated in the framework of the free ion approximation by diagonalization of the appropriate energy matrix. M.F. Reid’s f-shell empirical programs were used to evaluate the energy parameters. Only low energy levels (up to $35,000 \text{ cm}^{-1}$) were included in the calculations. The root mean square deviation between the experimental and calculated energies was 90 cm^{-1} .

Usually large fraction of the VUV d-f emission in fluorides activated with Er originates at the lowest (HS, $J = 8$) level [5]. Although some emission from the higher energy (LS, $J = 8$) state has also been observed its intensity was low due to competing processes of nonradiative relaxation to the lower lying doublet ($^2\text{F}_{5/2}$) or (HS, $J = 8$) states (the decay time was, correspondingly, very short) [5]. Er^{3+} activated BaF_2 is no exception as its

VUV emission is dominated by slow spin-forbidden transition between the lowest state (HS, $J = 8$) of the $4f^{10}5d$ configuration and the ground state $^4I_{15/2}$ of the $4f^{11}$ configuration [6].

Unexpectedly the emission from the $(\text{Ba,Lu})\text{F}_2:\text{Er}$ shows significant fast contribution under excitation into 157 nm (LS, $J = 8$) and 148 nm (LS, $J = 7$) bands at room temperature and under excitation into (LS, $J = 8$) 157 nm at 10 K (see Fig. 2). The fast component (thick solid trace in Fig. 2) shows three broad bands peaking at 216, 234 and 282 nm.

The emission spectrum under 148 nm (LS, $J = 7$) excitation at 10 K (Fig. 3) is very different, showing a number of sharp emission lines that are clearly due to $4f^{11}$ intraconfigurational transitions. Interestingly the spectrum shows also broad bands dominating the spectrum shown in Fig. 2 but, since the fast and slow traces overlap, the decay times of both the sharp lines and broad bands must be much longer than 190 ns (time between consecutive pulses from synchrotron).

The fast and slow emission bands and lines reported so far and shown in Figs 2 and 3, are supplemented by new bands revealed in spectra measured with the VUV monochromator and detector. In Figs 4 and 5 we present VUV/UV emission spectra measured under excitation at 157 nm into (LS, $J = 8$) excitation band and 148 nm into (LS, $J = 7$) excitation band. These spectra show that the VUV emission band at 162.5 nm contributes a significant fraction of the total VUV and UV emissions. It is interesting to note the weak broad band at 170 nm in the “slow” thin trace measured with a 150 ns delay and shown in Fig. 4. This emission is due to the spin-forbidden transition from the lowest high spin state of the $4f^{10}5d$ configuration (HS, $J = 8$). Usually in other fluorides, including BaF_2 , this band dominates the VUV emission from Er^{3+} ion.

The arrows in Figs 4 and 5 indicate the calculated positions of lines and bands that correspond to transitions terminating at the ground state $^4I_{15/2}$ and consecutive higher lying levels of the $4f^{11}$ configuration and originating at the $4f^{10}5d$ (LS, $J = 8$) level at $61,540\text{ cm}^{-1}$ (Fig. 4) and at the $^2G_{7/2}$ level of the $4f^{11}$ configuration at $66,140\text{ cm}^{-1}$ (Fig. 5). It is interesting to note a reasonably good agreement between the calculated (see Fig. 1) and experimental value of the $^2G_{7/2}$ level energy. Although we do not see the $^2G_{7/2}$ level directly, a good agreement between calculated and measured positions of large number of sharp emission lines makes a strong argument that we are indeed observing emissions starting at the $^2G_{7/2}$ level. This is, to the best of our knowledge, the highest lying emitting state of the $4f^{11}$ configuration of Er^{3+} ion in any solid state material. Since we are dealing with two different configurations, the transitions, radiative and nonradiative, between different states, may induce a significant change of the configuration coordinate (electron-phonon coupling) strongly modifying transition rates and energies. The best way to include these effects is by means of the configuration coordinate diagram, as shown in Fig. 6.

The positions of potential energy parabolas in Fig. 6, corresponding to various electronic states of the Er^{3+} ion have been calculated using experimental and calculated values of $4f^{11}$ electronic energies, and experimental absorption and emission peak energies for broad band transitions involving $4f^{10}5d$ states. Under linear approximation all the parabolas have the same curvature but may have different equilibrium (minimum) positions. We assume that there are two such positions, one for all relevant states of the $4f^{10}5d$ configuration and the second for the three key states of the $4f^{11}$ configuration, $^4I_{15/2}$ (the ground state), $^2F_{5/2}$ and $^2G_{7/2}$.

We note that, consequently, the minimum of the $^2F_{5/2}$ parabola is positioned above the minimum of the (LS, $J = 8$) parabola. It follows that the $^2F_{5/2}$ state is not at all likely to

facilitate energy transfer between these two states. Unless there is an efficient direct relaxation from the LS to the HS $4f^{10}5d$ states, the LS state, when excited, should decay radiatively to lower states of the $4f^{11}$ configuration. Any upward shift of the $4f^{10}5d$ parabolas (lower $10Dq$ or lower symmetry crystal field component responsible for the splitting of the e-states) may change situation; either the $^2F_{5/2}$ level may intercept the excitation energy from the LS state and emit, or it may enhance the energy transfer from the LS down to the HS state. So, the possible scenarios include emission from the LS state, emission from the $^2F_{5/2}$ state and emission from the HS state. Depending on the temperature and energy positions and/or barriers some mixed scenarios are also possible. The second scenario, emission from the $4f^{11}$ state, at least for low temperatures, occurs for the trio of higher energy levels, (LS, $J = 8$), (LS, $J = 7$) and $^2G_{7/2}$. For higher temperatures the energy relaxation down to the (LS, $J = 8$) state is possible so that the final result will be the fast spin-allowed emission from this level. We note that since the $^2G_{7/2}$ parabola intersects the (LS, $J = 7$) parabola almost exactly in its minimum, the efficient relaxation from that level (147 nm excitation band), down to the $^2G_{7/2}$ parabola, is very likely.

4. Conclusions

The fast and efficient emission from the LS $4f^{10}5d$ level, bypassing a HS $4f^{10}5d$ level of Er^{3+} ion in $(Ba,La)F_2$, has been observed. The substantial population of the higher LS level must be due to lack of efficient nonradiative relaxation to the lower lying HS level. Both levels are positioned below the $^2F_{5/2}$ level probably because of the additional lower symmetry crystal field component induced by interstitial fluorines needed to compensate massive La presence in the crystal.

At 10 K the fast emission (45 ns) can be excited by tuning the excitation light to cover the 157 nm band corresponding to the parity and spin-allowed transition from the ground state $^4I_{15/2}$ to the (LS, $J = 8$) state of the $4f^{10}5d$ configuration. Excitation into the second LS

band (at 148 nm) generates slow VUV and UV consisting mostly of the sharp lines originating at the $^2G_{7/2}$ level of the $4f^{11}$ configuration. At room temperature the decay time of the spin-allowed emission shortens (35 ns) and the fast emission follows excitation into any of the two LS bands ($J = 8$ and $J = 7$) covering the range between 140-150 and 152-160 nm.

We conclude that the highly lying levels of the $4f^{11}$ configuration actively participate in intraconfigurational $4f^{10}5d \rightarrow 4f^{11}$ transitions on the Er^{3+} ion shaping the emission spectra and decay times.

5. Acknowledgments

We are grateful to Prof. Alex Lempicki of Boston University, for donating crystals used in this study, Prof. Georg Zimmerer and Dr Gregory Stryganyuk of Hasylab for help and hospitality during Superlumi experiments, Prof. M.F. Reid of Canterbury University, Christchurch, New Zealand for his f-shell empirical programs to calculate lanthanide $4f^{11}$ energy levels.

We also acknowledge DESY and EC for support during Superlumi experiments under Contract RII3-CT-2004-506008 (IA-SFS).

6. References

- [1]. R.T. Wegh, E.V.D. van Loef, G.W. Burdick and A. Meijerink, Mol. Phys. 101 (2003) pp. 1047-1056.
- [2]. G. Zimmerer, Nucl. Instr. Meth. Phys. Res. A 308 (1991), p. 178.
- [3]. http://hasylab.desy.de/facilities/doris_iii/beamlines/i_superlumi/index_eng.html
- [4]. L. van Pieterse, M.F. Reid, G.W. Burdick, and A. Meijerink, Phys. Rev. B 65 (2002) pp. 0451141-04511413.
- [5]. R.T. Wegh and A. Meijerink, Phys. Rev. B 60 (1999) pp. 10820-10830.
- [6]. A.J. Wojtowicz, Optical Materials, accepted for publication.

Accepted manuscript

FIGURE CAPTIONS

Fig. 1 The excitation spectrum of the $^4S_{3/2} - ^4I_{15/2}$ emission in $(\text{Ba,Lu})\text{F}_2:\text{Er}$ at 10 K. The emission wavelength was 550 nm, the resolution was 0.32 nm. The broad bands at 157, 148 and 138 nm are due to the spin-allowed transitions from the ground state, $^4I_{15/2}$, to quartet states of the $4f^{10}5d$ configuration. The J values indicate the state of the $4f^{10}$ core coupled to a 5d electron occupying the lowest crystal field state.

Fig. 2. Time gated emission spectra of $(\text{Ba,Lu})\text{F}_2:\text{Er}$ under 157 nm excitation into the (LS, J = 8) band at 10 K. Solid thick trace presents fast emission (no delay, 40 ns gate) while the thin solid trace presents slow emission (150 ns delay, 40 ns gate). Note and disregard the fast second order contribution at 430 and 470 nm. The resolution was 1.35 nm.

Fig. 3. Time gated emission spectra of $(\text{Ba,Lu})\text{F}_2:\text{Er}$ under 148 nm excitation into the (LS, J = 7) band at 10 K. Thick solid trace presents fast emission (no delay, 40 ns gate) while the thin solid trace presents slow emission (150 ns delay, 40 ns gate). The resolution was 1.35 nm.

Fig. 4 Time gated VUV and UV emission spectra of $(\text{Ba,Lu})\text{F}_2:\text{Er}$ under 157 nm excitation into the (LS, J = 8) band at 10 K. Thick solid trace presents fast emission (no delay, 40 ns gate) while the thin solid trace presents slow emission (150 ns delay, 40 ns gate). The resolution was 1.1 nm. Arrows indicate the positions of emission bands originating at the (LS, J = 8) state of the $4f^{10}5d$ configuration and terminating at the $^4I_{15/2}$ ground state and consecutive states of the $4f^{11}$ configuration. Note the slowly decaying weak band at 170 nm, presumably due to the spin forbidden transition starting at the (HS, J = 8) $4f^{10}5d$ state.

Fig. 5. Time gated VUV and UV emission spectra of $(\text{Ba,Lu})\text{F}_2:\text{Er}$ under 148 nm excitation (LS, J = 7) at 10 K. Thick solid trace presents fast emission (no delay, 40 ns gate) while the thin solid trace presents slow emission (150 ns delay, 40 ns gate). The resolution was 1.35 nm. Broken trace presents slow VUV emission measured with resolution of 1.1 nm. There is almost no difference between slow and fast traces. Arrows indicate the positions of emission bands originating from the $^2G_{7/2}$ level and terminating at various levels of the $4f^{11}$ configuration.

Fig. 6. Schematic configuration coordinate diagram showing higher excited states of Er^{3+} ion. The equilibrium position of $4f^{11}$ states, including the ground state $^4I_{15/2}$ and two important states, $^2F_{5/2}$ and $^2G_{7/2}$, is at zero, the equilibrium positions of $4f^{10}5d$ levels were shifted to fit experimental transition energies (from excitation and emission spectra). The diagram suggests possibility of emission from the $^2G_{7/2}$ and no radiative nor nonradiative contribution from the $^2F_{5/2}$ levels.

Figure 1:

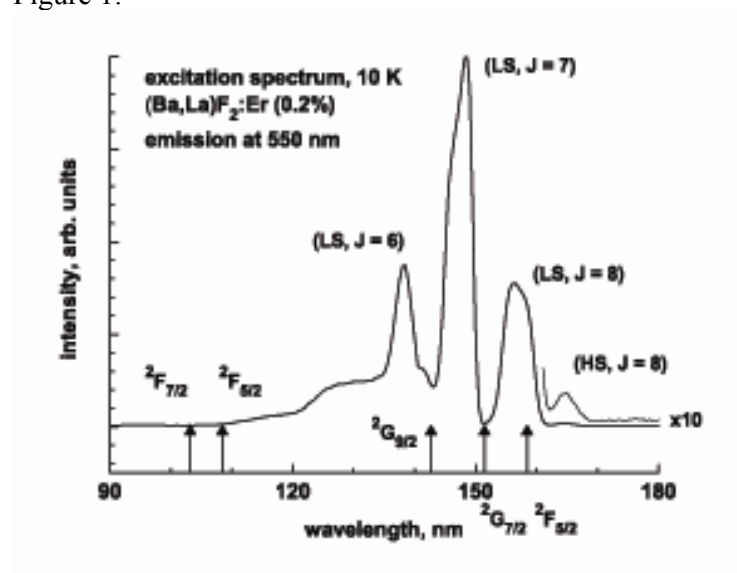


Figure 2:

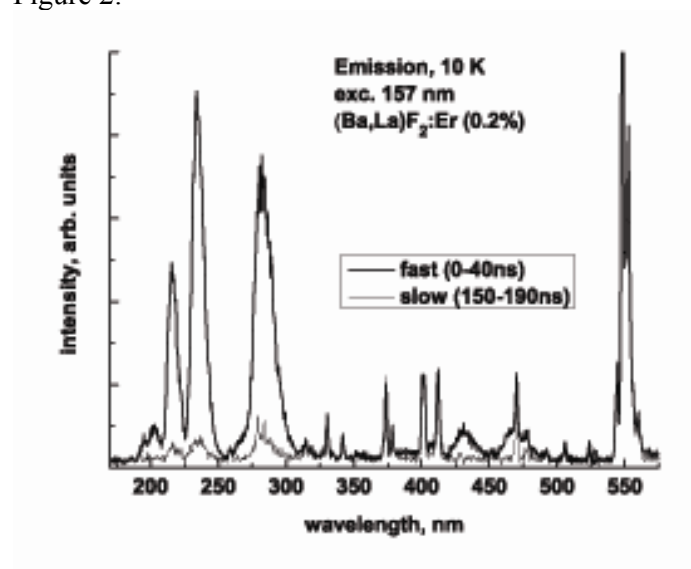


Figure 3:

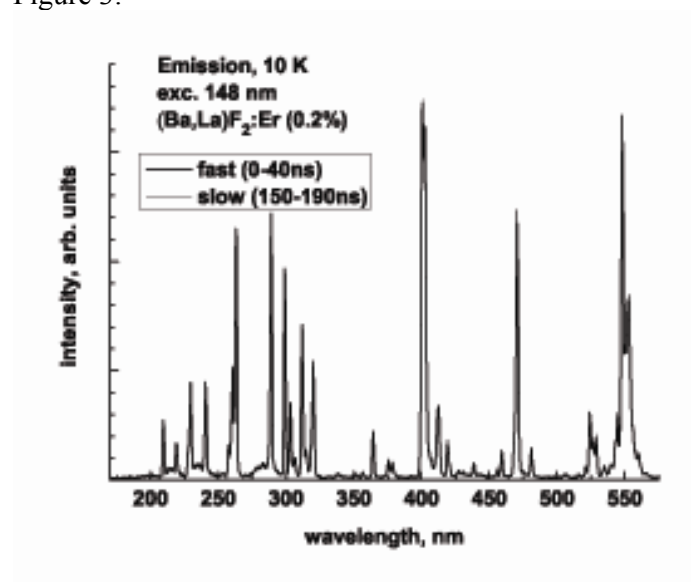


Figure 4:

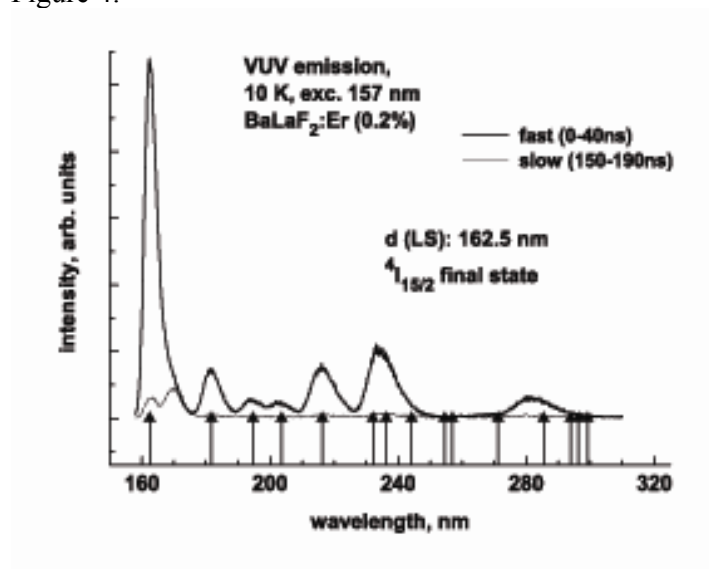


Figure 5:

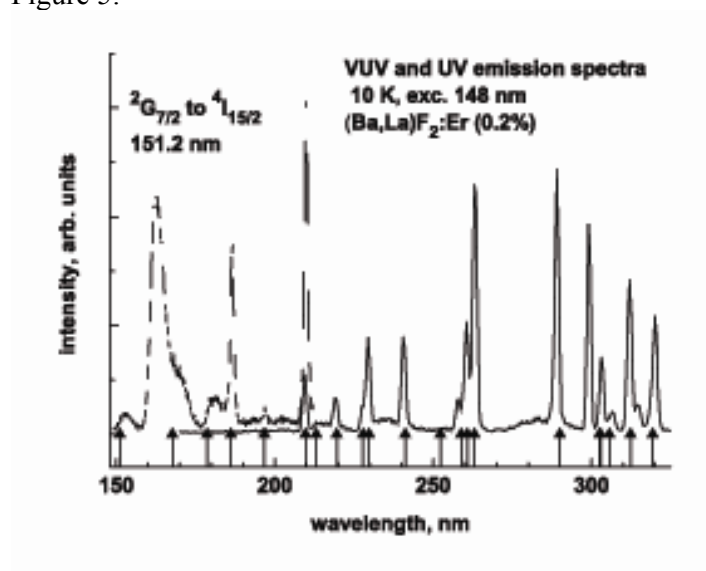


Figure 6:

